JOURNAL OF APPLIED ELECTROCHEMISTRY 14 (1984) 627–638

Distribution of local mass transfer coefficients over one electrode bombarded by submerged multijets of electrolyte

J. O. NANZER, F. COEURET*

CNRS–ENSCR, Avenue du Général Leclerc, 35000 Rennes-Beaulieu, France

Received 15 August 1983, revised 6 December 1983

This work deals with the experimental study of the distribution of local mass transfer coefficients and local shear stresses over a circular disc bombarded by submerged multijets of electrolyte. The influence of the geometrical and hydrodynamical parameters is examined. From visualization of the impingement of free multijets, an interpretation of the distributions is attempted.

1. Introduction

The conclusion of Coeuret [1] suggested that the electrochemical method for the determination of mass transfer coefficients could be advantageously used when multijets impinge an electrode. This is reasonable owing to the possibility of multijets being used for mass transfer enhancement in electrochemical cells. An electrode impinged by multijets may accept high current densities. Moreover, the spatial distribution of the local mass transfer coefficients may be uniform, at least for a sufficiently high number of ordered jets. The overall mass transfer between multijets and planar electrodes was studied by Nanzer *et al.* [2] as a function of most of the measurable parameters and a very satisfactory empirical correlation was proposed for a class of experimental conditions. It was shown that, from an overall point of view, the electrodes are pseudo-uniformly accessible when their diameters are smaller than the diameter of the zone impacted by the jets.

The overall heat or mass transfer between liquid submerged multijets and a wall has been studied by various authors [3–10], although the study by Nanzer *et al.* [2] seems to have been one of the first works using the electrochemical method. On the contrary, it seems that no paper has been concerned with the experimental distribution of local coefficients for impinging multijets. Concerning the impact of a single jet, the recent work of Kataoka *et al.* [11] deserves mention because it appears to be the first using the electrochemical method for the determination of the distribution of local mass transfer coefficients over the surface receiving the jet. At the same time, Kataoka *et al.* [11] present measurements of local wall velocity gradients.

The aim of the present work is to continue previous work [2] through the determination of local mass transfer coefficients and local wall shear stresses over a planar circular surface impinged by several classes of rows of jets. In spite of the complexity, interesting information could be obtained from such a local experimental study.

2. Experimental

The hydraulic circuit and the measuring cell are the same as those previously described in detail by Nanzer *et al.* [2]. The electrolyte is maintained at 30° C and flows in a closed circuit. This electrolyte is a solution of 0.5 M NaOH which acts as a conducting support for a mixture of potassium ferricyanide (5×10^{-3} M) and of potassium ferrocyanide (5×10^{-2} M). For the experimental conditions the molecular diffusion coefficient of the ferricyanide ion is $D = 8.8 \times 10^{-6}\,cm^2\,s^{-1}$, the kinematic viscosity of the electrolyte is $\nu = 0.0094\,cm^2\,s^{-1}$ (the Schmidt number $Sc = \nu/D$ is 1070) and the specific gravity of the electrolyte is $\rho = 1.05\,g\,cm^{-3}$.

Fig. 1a is a schematic view of the part of the cell containing the electrodes and in which the jets of electrolyte are formed. The liquid flows from the upper part of the cell successively through the

*Present address: Facultad de Ingenieria Quimica UNL, 3000 Santa Fe, Republic of Argentina.

0021–891X/84 $03.00 + .12

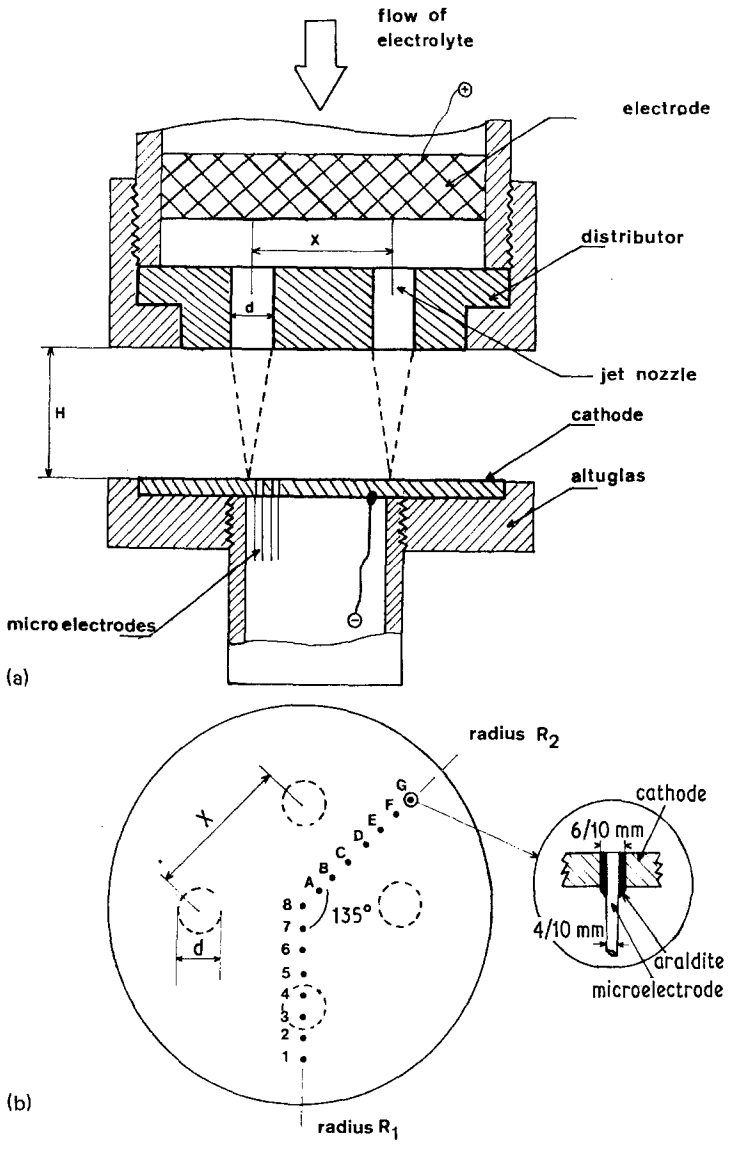

Fig. 1. Schematic view of the cathode.

anode (knit of nickel wire with a total surface area of about 2000 cm^2) and the distributor (thickness 2 cm) having N holes of diameter $d = 0.25$ cm is arranged according to a square array of side X (Fig. 1b). The following distributors, defined as previously by Nanzer *et al.* [2], have been used:

Distributor	N	X (cm)
P5	4	2.5
P6	9	1.66
P7	16	1.25
P8	25	1.0
P9	36	0.833

The hole diameter $d = 0.25$ cm is common to all the distributors; this value of d corresponds to the empirical correlation established earlier [2]. The distance H between the nozzles and the transfer surface is chosen such that H/d is equal to 2, 4 or 6; the maximum value of 6 is adopted according to the previous results which show that $\bar{k}$ (the mass transfer coefficient) is nearly independent of H/d when $H/d < 6$–8 [1, 2]. Thus, the maximum value of H is 1.50 cm which is sufficiently small compared with the distance (5.0 cm) between the electrode periphery and the wall of the cylindrical chamber containing the test section of Fig. 1a, for the influence of that wall to be negligible. The

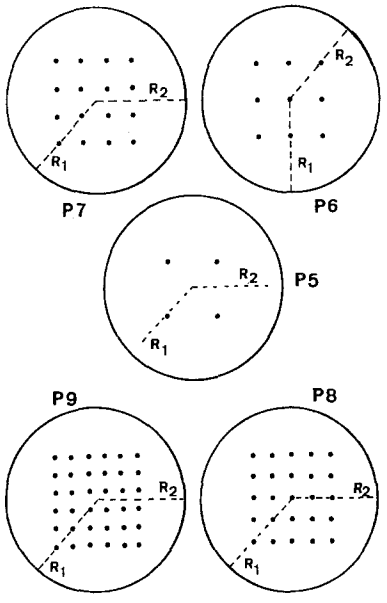

Fig. 2. Different distributors and situations of the radii R_1 and R_2 with respect to the distributors.

Reynolds number $Re = u \cdot d/\nu$, where u is the mean exit velocity of the jet, is also varied.

The cathode (Fig. 1a) receives the jets and acts as the transfer surface, the mass transfer coefficients being measured by means of the electrochemical reduction of ferricyanide ions. It consists of a circular disc of copper (diameter 9 cm, thickness 0.5 cm) which is successively gold and platinum plated. As for the electrodes used earlier [2], this cathodic disc is supported by a piece of plexiglass the axis of which is the cell axis.

This cathode contains 15 microelectrodes disposed along two radii R_1 and R_2 at 135° (see Fig. 1b) and are respectively numbered from 1 to 8 (Electrode 8 occupies the centre of the disc) and then from A to G. As shown in the detail of Fig. 1b, each microelectrode consists of a 0.4 mm diameter platinum wire held in a hole of diameter 0.6 mm through the thickness of the disc; the platinum wire is isolated from the disc by an araldite film. The centres of the two successive microelectrodes are separated by a distance of 0.5 cm; microelectrodes 1 and G are situated at a distance of 1.0 cm from the periphery of the disc. After the installation of the microelectrodes, the copper disc is gold plated (hard Au–Co deposit) and then platinum plated. Fig. 2 shows the five distributors P5 to P9 and specifies the position of the radii R_1 and R_2 (along which the microelectrodes are situated) with respect to the jet nozzles. The electrical circuit is a classical 3-electrode polarographic circuit using a PRT 20-2X TACUSSEL potentiostat.

As in previous works [12, 13], such microelectrodes allow two types of measurements: (a) 'in reactive wall' measurements and (b) 'in inert wall' measurements.

2.1. *'in reactive wall' measurements*

The circular disc and a given microelectrode are electrically connected and maintained at a cathodic potential corresponding to the diffusional limitation of the ferricyanide ions. The limiting diffusion current I_d which corresponds to the reaction on the microelectrode is measured; it leads to the local value k of the mass transfer coefficient, i.e.:

$$k = \frac{I_d}{z \cdot F \cdot S \cdot C_s} \tag{1}$$

where z is the number of electrons in the electrode reaction ($z = 1$), F is the Faraday number, S the microelectrode surface area and C_s the ferricyanide concentration in the bulk of the solution (C_s is known by amperometric titration with cobalt sulphate). Such a determination of k is made for each microelectrode. The overall current I corresponds to the overall mass transfer coefficient $\bar{k}$ at the whole electrode (the fractional surface area occupied by all the microelectrodes is negligible when compared to the surface of the cathodic disc).

2.2. *'in inert wall' measurements*

The circular cathodic disc is not electrically connected to the measuring circuit. Only the microelectrodes are successively used as cathodes in the polarographic circuit, thus allowing the measurement of diffusional local currents I'_d which lead, through a relation similar to Equation 1, to the corresponding local coefficients k', such as:

$$k' = 0.807 \cdot \frac{D^{2/3} \cdot s^{1/3}}{d^{1/3}} \tag{2}$$

Expression 2 results from the solution of the diffusion–convective equation for mass transfer towards a circular microelectrode of diameter d embedded in an inert wall [14]. In Equation 2 s is

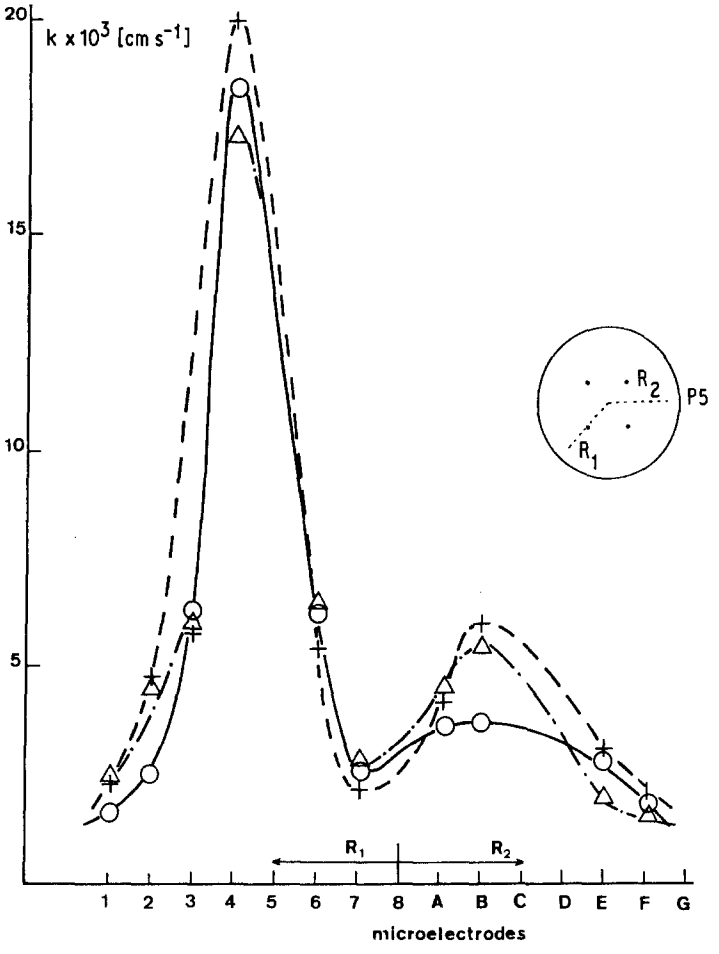

Fig. 3. Distribution of k along R_1 and R_2. Distributor P5; $Re = 3260$; H/d values of 6 – +, 4 – △; 2 – ○.

the wall velocity gradient $(\partial u/\partial y)_{y=0}$ (y is the normal to the wall and u the velocity component parallel to the surface; for a newtonian fluid, s is related through $\tau = \mu \cdot s$ to the local wall shear stress τ and to the dynamic viscosity μ).

3. Experimental results

3.1. *Radial distributions of local mass transfer coefficients*

Fig. 3 gives the distributions of k along both radii R_1 and R_2 for distributor P5, $Re = 3260$ and three values of H/D. One sees that these distributions are highly nonuniform, the deviation from uniformity depending on the position of the microelectrodes with respect to the axis of the jets. [See detail of Fig. 3 this position for distributor P5]. In the case of Fig. 3, the point of impact of a jet is along the radius R_1 between microelectrodes 4 and 5; in the distribution of k such an impact corresponds to an accentuated maximum.

Along the radius R_2 which is equidistant from the four jets, the distribution of k is more uniform, with a less prominent maximum lying between microelectrodes A and D. In Fig. 3, the influence of H/d on k seems to be small, but the conclusions are different with other distributors for which a decrease of k is noticeable when $H/d > 4$ [15].

Fig. 4 compares the distributions of k obtained for $H/d = 6$ and three values of Re for distributor P5. When Re increases and the regime is changing from laminar to turbulent, the position of the main maximum is unchanged but its amplitude is increased. Regarding the second maximum, situated along R_2, one notes that its amplitude increases with Re, but such an increase is smaller than for the first maximum.

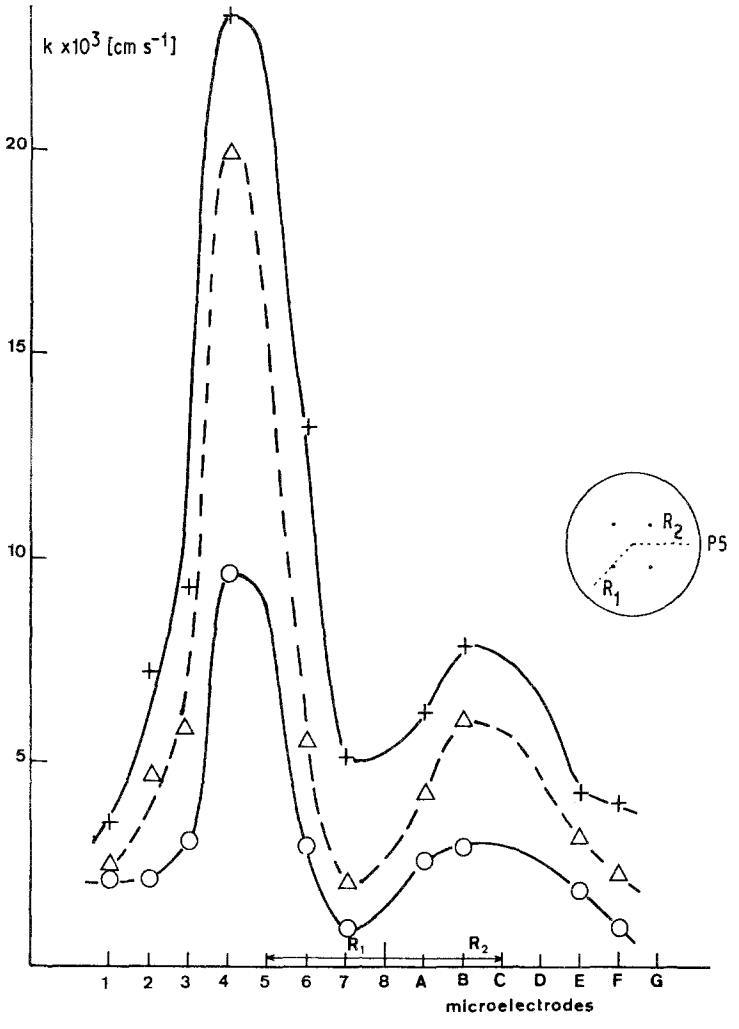

Fig. 4. Distribution of k along R_1 and R_2. Distributor P5; $H/d = 6$; Re values of 1570 – ○; 3260 – △; 4720 – +.

The distributions obtained using various distributors are compared in Figs. 5 and 6; due to the change in the distance X between the holes, the maxima move on passing from one distributor to another. The forms of the distributions are similar to those obtained with distributor P5, except that the number of maxima along R_1 depends on the distributor. For distributor P5, there is a maximum between microelectrodes 4 and 5; for distributor P7, there exist two maxima (around microelectrodes 3 and 6) which correspond to the impact of two jets; for distributor P9 there are three maxima corresponding to the impact of three jets around microelectrodes 2, 4 and 7. Regarding the distribution of k along R_1, one sees that, for H/d = constant and $Re \approx$ constant, as a consequence of the decrease of the distance X between the jets there is an increase of the mass transfer coefficient. If the distributions established with P5 (4 jets) and with P9 (36 jets) are compared, it is seen that the sinusoidal form of the distribution presents oscillations between peaks and valleys which are smaller for P9 than for P5.

Concerning the distribution along R_2 (electrodes no. 8, and A to G), this has only one flat maximum for any distributor among P5, P7 and P9. Indeed, the microelectrodes along R_2 are situated between two lines of identical jets (see Fig. 2). It is observed that the higher the number of jets in a row, the more marked is the increase of the amplitude of the flat maximum with the Reynolds number Re; on the contrary, when Re is constant, this amplitude is nearly independent of H/d. This observation may be imputed to the fact

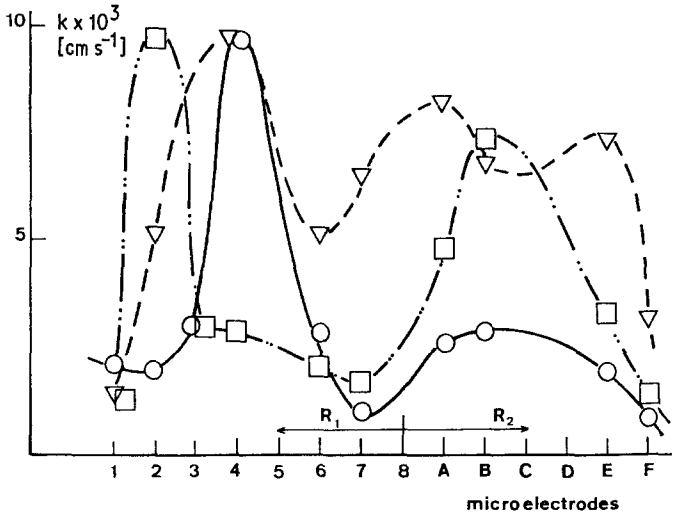

Fig. 5. Distribution of k along R_1 and R_2 – comparison of different multi-jets. $H/d = 6$; distributor P5 – ○; P6 – ▽; P8 – □.

that, as N increases X decreases; the consequence is the reduction of the inter-jet space width, the axis of which is radius R_2, and thus the improvement of the mean electrolyte flow velocity in that space.

Distributions deduced for P6 and P8 may be particular owing to the fact that both radii R_1 and R_2 are directly bombarded by the jets; for P6, 3 maxima (near microelectrodes no. 5, 8 and E) are expected and for P8 the distributions would present 5 maxima (near microelectrodes no. 2, 5, 8, B and D). Fig. 5 shows that for P8 this was not demonstrated, but microelectrodes no. 5, 8, C and D were not available because they were short-circuited with the circular disc; only the maximum corresponding to microelectrode no. 2 is clearly shown.

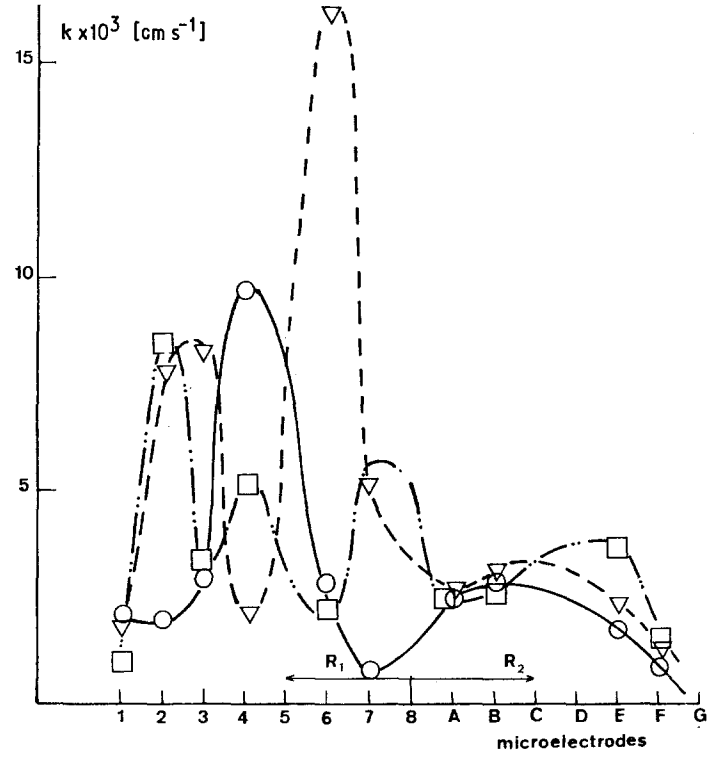

Fig. 6. Distribution of k along R_1 and R_2 – comparison of different multi-jets. $H/d = 6$; distributor P5 – ○; P7 – ▽; P9 – □.

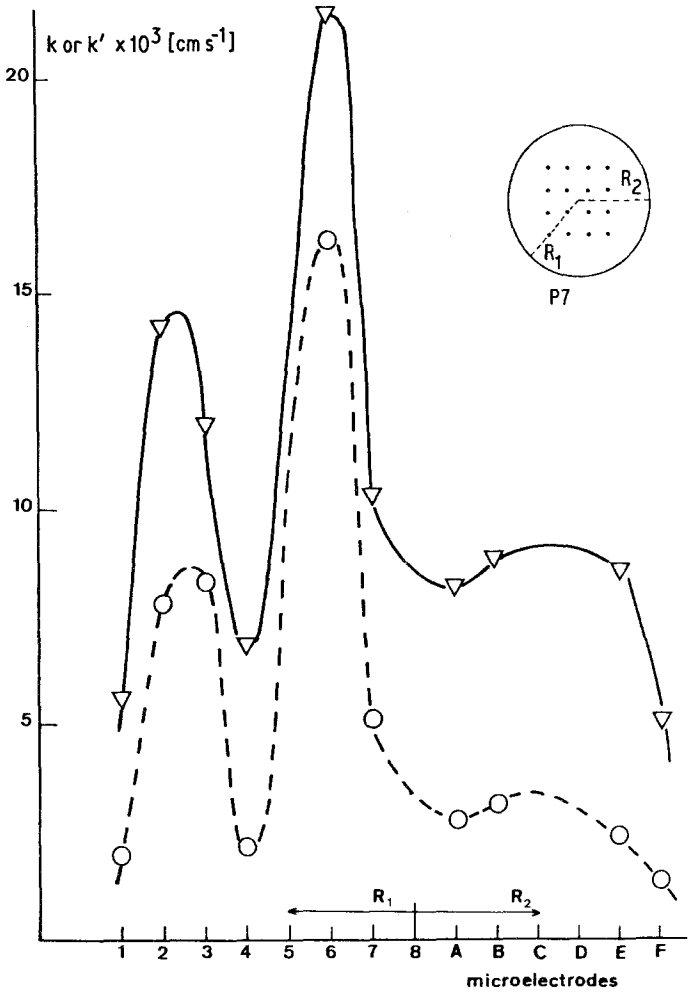

Fig. 7. Comparison of the distribution of k and k' over the transfer surface. Distributor P7; $Re = 1300$; $H/d = 6$.

3.2. *Mass transfer and momentum transfer*

The determinations of k and k' at the same place on the transfer surface for various experimental conditions allow a comparison of the corresponding spatial distributions of k and k'. Many graphical comparisons have been made previously [15] but here only Fig. 7 is given in order to illustrate the results obtained. One observes that the distributions of both k and k' are similar according to the analogy between mass transfer and momentum transfer.

The spatial distributions of k and k' are of a sinusoidal type; effectively, the ratio k/k' is also distributed in a sinusoidal manner (Fig. 8). One may attempt to use the local experimental data k and s to test the Chilton–Colburn analogy which expresses, for high Schmidt numbers, the analogy between mass and momentum transfer [16]. This analogy is written as follows:

$$\frac{k}{V} \cdot Sc^{2/3} \equiv \frac{\mu \cdot s}{\frac{1}{2} \cdot \rho \cdot V^2} \tag{3}$$

where V represents a characteristic velocity of the flow, generally the mean flow velocity. The local hydrodynamic state (see later in Fig. 11 which shows visualizations) is so different from one location to another over the transfer surface that it is not possible to choose a velocity characterizing all the flow.

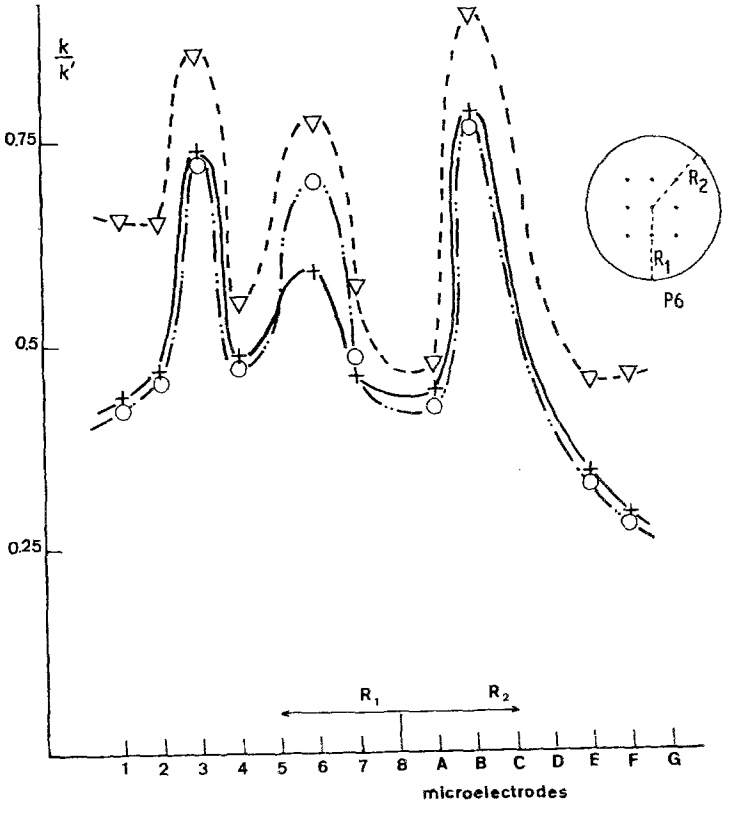

Fig. 8. Variations of k/k' along R_1 and R_2. Distributor P6; *Re* values of 1300 – ○; 1700 – +; 3100 – ▽.

The relation between k and k' is investigated in Fig. 9 for distributor P5; all the functioning microelectrodes in various experimental conditions are included. The correlation coefficient of the empirical correlations which could be plotted for each *Re* varies between 0.92 and 0.98; this signifies that the deviation of the linearity between k and k' is small, in spite of the fact that all the microelectrodes are supposed to have the same reactive surface area, equal to the cross sectional area of the 0.4 mm diameter platinum wire. However, this approximately linear relation between k and k' is not general [15].

3.2. *Mean mass transfer coefficients*

The mean mass transfer coefficient is obtained in two ways:

(a) on the one hand, $\bar{k}_{exp}$ which is obtained through Equation 1 from the experimental intensity I of the limiting diffusional current at the total surface area of the circular disc (diameter 9 cm). I is measured during the experiments with a 'reactive wall' (Fig. 1).

(b) on the other hand, $\bar{k}_{calc}$ which is the mean value of k along R_1 and R_2.

Fig. 10 compares both coefficients $\bar{k}_{exp}$ and $\bar{k}_{calc}$ for various experimental conditions (distributors P5 and P8; three values of H/d). An approximately linear relation exists between $\bar{k}_{exp}$ and $\bar{k}_{calc}$ but the ratio $\bar{k}_{calc}/\bar{k}_{exp}$ is higher than 1. This ratio is synonymous with the ratio A_{eff}/A_{exp} of electrode surface areas. [A_{exp} = true area (63.6 cm^2) of the circular disc; A_{eff} = surface area of the circle which would contribute practically to all the diffusional mass transfer (the difference $A_{exp} - A_{eff}$ has a negligible contribution).]

The slope of the least-square straight line plotted in Fig. 10 is 1.94 so that A_{eff} corresponds to a circle of diameter 6.5 cm. The system behaves as if nearly all the diffusional mass transfer takes place in this circle, in agreement with the conclusion of Nanzer *et al.* [2] concerning the experimental variation of the overall mass transfer

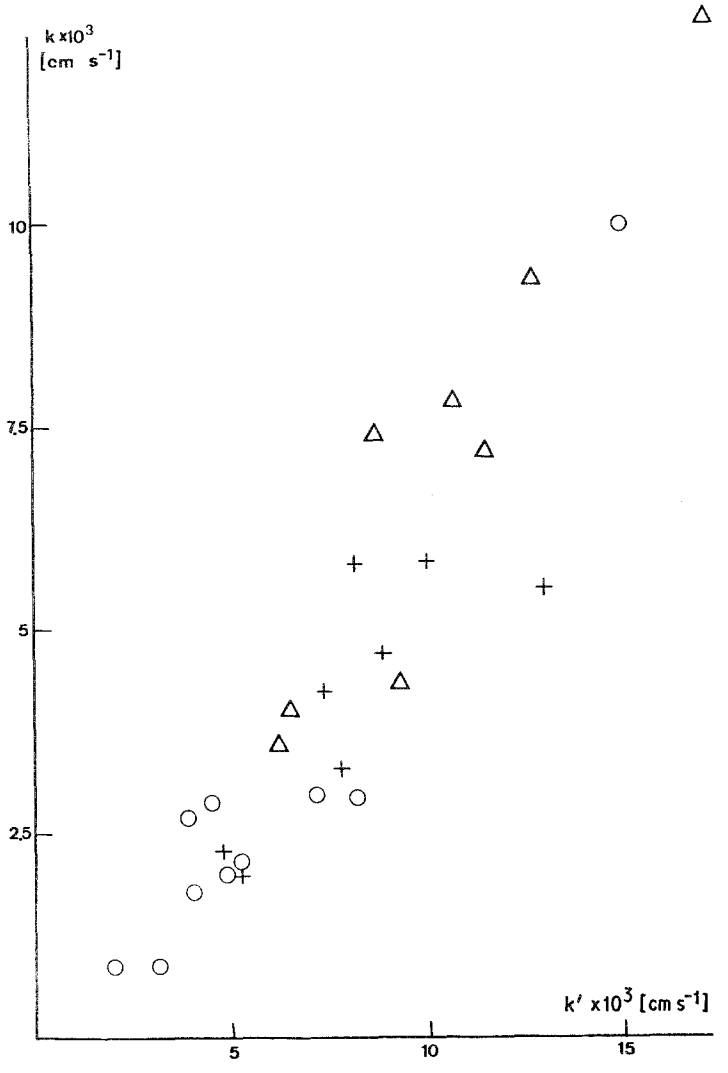

Fig. 9. Variations of k with k' for distributor P5. $H/d = 6$; Re values of 1570 – ○; 3270 – +; 4720 – ▽.

coefficient $\bar{k}$ with the diameter of the circular electrode (depending on the distributor used, $\bar{k}$ falls rapidly when the diameter is higher than 6.3 to 6.9 cm). The distributions of k (Figs. 3–7) also show that beyond microelectrodes 1 and F, which are situated at a distance to the centre of the disc of 3.5 and 3.0 cm respectively, the value of k falls rapidly to zero.

4. Discussion

From overall mass transfer results it was concluded earlier [2] that the distribution of local mass transfer coefficients could be pseudo-uniform on the fraction of surface receiving the jets. Here, the existence of this well-defined fraction of surface area below the jets is confirmed. However, from local mass transfer determinations, which lead to the tertiary current distribution on the electrode bombarded by the jets, very important deviations from spatial uniformity are observed. The more numerous and adjacent are the jets (as in the case of distributor P9), the more uniform is the distribution.

Local values of k have been measured along radii R_1 and R_2 only: R_1 is along the diagonal of the square arrangement of the jets while R_2 is either below a line of jets, or in the middle between two rows of jets. Although possible, measurements along other radii would have been

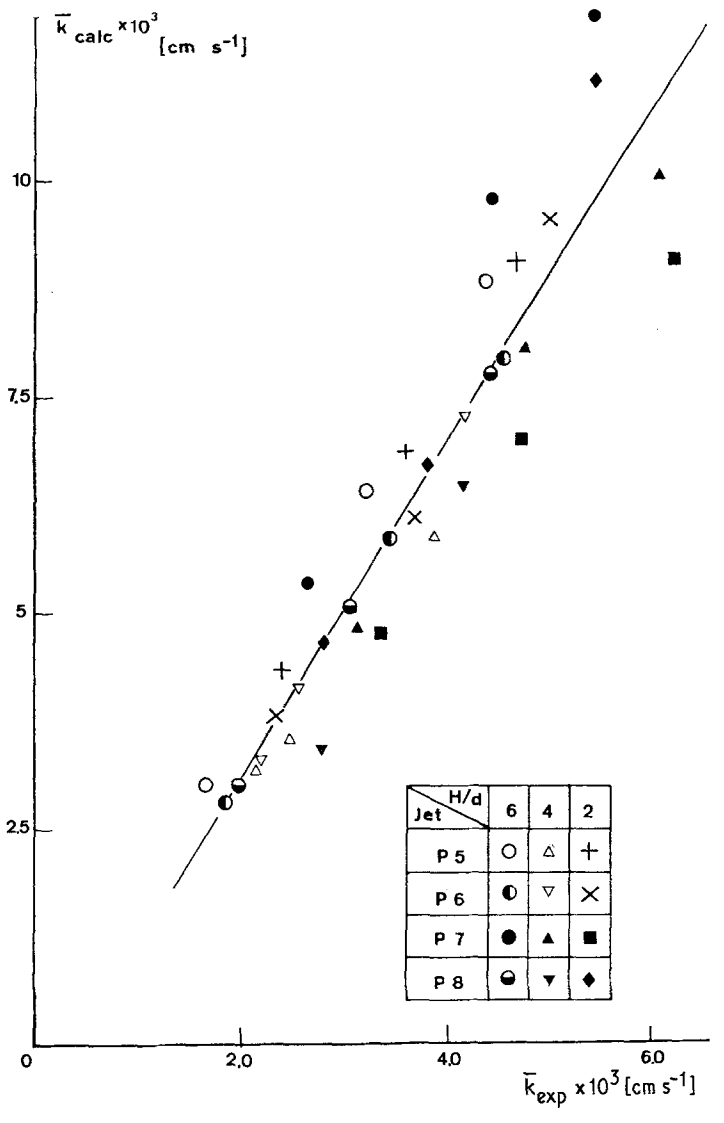

Fig. 10. Comparison of $\bar{k}_{calc}$ and $\bar{k}_{exp}$.

superfluous owing to the complexity of the hydrodynamics of the systems used.

Visualization of the structures originated by the impact of multijets has been observed using free multijets with relative distances H/d sufficiently high in order to avoid deformation of the structures. Fig. 11a (reproduced from a photo) represents the flow structure when the transfer surface is bombarded by free jets issued from distributor P5. This structure is characterized by the existence of a central elevated part with a dome-like form, the height of which is a function of the exit velocity of the jets, and by four arms normal to the sides of the square. These arms allow the liquid proceeding from the dome to be evacuated. The dome is produced by the colliding wall jets.

In our mass transfer experiments these flow structures are probably highly deformed, especially for very small H/d values; however, the structure of Fig. 11a may explain the form of the distributions of local mass transfer coefficients. For Figs. 3 and 4, for example, the radius R_1 crosses the jet impingement region and the neighbouring area where there is a wall jet flow. The smaller maximum would correspond to the boundary between the evacuation arm along R_2 and the

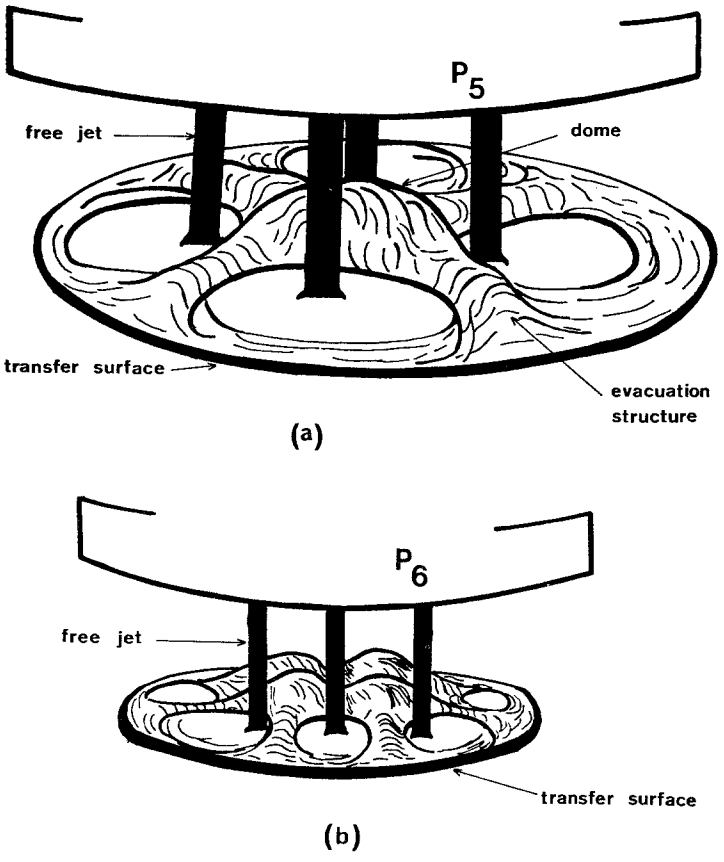

Fig. 11. Visualizations with free jets: (a) case of 4 jets; (b) case of 9 jets.

dome, the vertical of the top of which corresponds to a minimum of k.

The visualization carried out with distributor P6 (9 jets) is represented in Fig. 11b. In the middle of each square defined by the jets, a dome similar to that observed with distributor P5 (Fig. 11a) is present. Furthermore, between each row of jets a structure for the evacuation of the liquid exists. Fig. 11b allows the interpretation of the distribution of local coefficients k given in Fig. 5 for $H/d = 6$. Qualitatively, Fig. 11 can be compared with the results obtained by Gardon and Cobonpue [17] during the visualization of the distribution of heat transfer coefficients on a surface bombarded by multijets of air. More recently, the work of Goldstein and Timmers [18] used heat-sensible liquid crystals for the visualization of iso-heat transfer coefficient curves; the experiments used multijets of air impinging a planar surface in which liquid crystals were incorporated. As in these two works [17, 18], a maximum for the transfer coefficient is observed around the impingement point of the jets together with a depression or valley where the mass transfer is minimum; this last zone corresponds to the dome previously mentioned.

In this study it has not been possible to examine the influence of the fractional perforated area of the distributor since there is not always coincidence between a microelectrode and the axis of a jet. For this latter reason the values of the local mass transfer coefficients obtained with various distributors are not always quantitatively comparable and erroneous or contradictory interpretations could result from a comparison.

From an electrochemical engineering standpoint, the important variations between the local coefficients over a given electrode are worthy of note. As a conclusion of the 36 cases experimentally examined [15] it can be said that the local mass transfer coefficient is maximal around the impingement jet region and then falls rapidly. As the number N of jets is increased (or X is decreased), the uniformity is improved without being perfect. The existence of different but well-defined structures between the impingement zones of the multijets is responsible for the form of the

distributions. An increase of the uniformity of the distribution results from an increase of N and/or from a decrease of X. Finally, mass transfer between a row of jets and a surface depends, not only on the impact of the jets themselves, but also on the evacuation of the liquid from the transfer surface.

5. Conclusions

The distribution of the local mass transfer coefficients over an electrode bombarded by rows of submerged multijets depends strongly on the organization of the rows. In order to improve the accessibility of the electrode, the jets have to be narrow and closely spaced.

Acknowledgements

This work was carried out within the programme of scientific co-operation between France and Argentina. J. Nanzer gratefully acknowledges financial support from the French Government.

References

[1] F. Coeuret, *Chem. Eng. Sci.* **30** (1975) 1257.
[2] J. Nanzer, A. Donizeau and F. Coeuret, *J. Appl. Electrochem.* **14** (1984) 51.
[3] D. T. Chin and C. H. Tsang, *J. Electrochem. Soc.* **125** (1978) 1461.
[4] C. J. Chia, F. Giralt and O. Trass, *Ind. Eng. Chem. Fundam.* **16** (1977) 28.
[5] F. Giralt and O. Trass, *Can. J. Chem. Eng.* **53** (1975) 505.
[6] *Idem, ibid.* **54** (1976) 148.
[7] M. Korger and F. Krizek, *Int. J. Heat Mass Transfer* **9** (1966) 337.
[8] J. C. Bazan, S. L. Marchiano and A. J. Arvia, *Electrochim. Acta* **12** (1967) 821.
[9] J. Yamada and H. Matsuda, *Electroanal. Chem. Interfacial Electrochem.* **44** (1973) 189.
[10] B. Subba Rao, M. S. Krishna and G. J. V. Jagannadha Raju, *Period. Polytech. – Chem. Eng. (Budapest)* **17** (1973) 185.
[11] K. Kataoka, Y. Kamiyama, S. Hashimoto and T. Komai, *J. Fluid Mech.* **119** (1982) 91.
[12] A. Storck and F. Coeuret, *Electrochim. Acta* **22** (1977) 1155.
[13] D. Hutin, A. Storck and F. Coeuret, *J. Appl. Electrochem.* **9** (1979) 361.
[14] F. Coeuret and J. Legrand, *Electrochim. Acta* **28** (1983) 611.
[15] J. Nanzer, thesis, University of Rennes (1983).
[16] T. H. Chilton and A. P. Colburn, *Ind. Eng. Chem.* **26** (1934) 1183.
[17] R. Gardon and J. Cobonpue, 'Heat Transfer. Proceedings of the Second International Heat Transfer Conference', ASME, New York (1962) 454–60.
[18] R. J. Goldstein and J. F. Timmers, *Int. J. Heat Mass Transfer* **25** (1982) 1857.